Tone Reservation and Trellis Partial Transmit Sequences

Werner Henkel†, Steffen Trautmann‡, Valentin Zrno, Prashant Aggarwal

† International University Bremen
Bremen, Germany
E-mail: w.henkel@iu-bremen.de

‡ In neon Technologies Villach AG
Villach, Austria
E-mail: Steffen.Trautmann@in neon.com

***Abstract*— After shortly computing the error probability caused by clipping, we give some details on "Tone Reservation" and "Trellis Partial Transmit Sequences" for peak reduction and provide new simulation results.**

I. Introduction

Clipping is of major concern in multicarrier systems. It causes out-of-band noise and increased error rates. To begin with, we rst give a result of the error rate caused by a clip. The overall symbol-error rate will then be

$$P(\text{symb err}) = P(\text{symb err}|A)P(A) + P(\text{symb err}|A^c)P(A^c), \quad (1)$$

where A is the clipping event and A^c is the non-clipped case (see [1]). The bit-error probabilty follows to be $P(\text{bit err}) \approx 1/\log_2(M) \cdot P(\text{symb err})$ for Gray coding or $P(\text{bit err}) \leq 1/2 \cdot P(\text{symb err})$ as a rough bound for other mappings. The symbol-error probability for an M-point QAM constellation is given by

$$\begin{aligned} &P(\text{symb err}|\text{clip}) = \\ &\tfrac{1}{M}\Big[\Big(M - 4\cdot(\sqrt{M}-2) - 4\Big)\cdot(4\cdot P_{th} - 4\cdot P_{th}^2) \\ &+ 4\cdot(\sqrt{M}-2)\cdot(3\cdot P_{th} - 2\cdot P_{th}^2) \\ &+ 4\cdot(2\cdot P_{th} - 1\cdot P_{th}^2)\Big] \end{aligned} \quad (2)$$

with

$$P_{th} = Q\left(\left[\frac{3\sqrt{N}\pi l^2}{\sqrt{2(M-1)}}\right]^{\frac{1}{3}}\right) . \quad (3)$$

and $Q(x) = 1/2 \cdot \text{erfc}(x/\sqrt{2})$. l and N are the clipping level normalized to the standard deviation and the number of carriers, respectively. Note that the subtraction of the quadratic terms P_{th}^2 is required to eliminte double-counted areas from two intersecting thresholds. The rst line of (2) relates to the inner points, the second line to the edges, excluding the corner points, and the third line corresponds to the corner points. Equations (2) and (3) result from corrections of [1], detailed in [2]. Bahai et al. derived in [1] the probability P_{th} to exceed the threshold as

$$P_{th} = Q\left(d^{1/3}/\sigma\right) \quad (4)$$

with a point spacing of $2d$. According to [2], σ and d should correctly[1] be

$$\sigma = \left(\frac{1}{\sqrt{3N}\pi l^2}\right)^{\frac{1}{3}} , \quad d = \sqrt{\frac{3}{2(M-1)}} . \quad (5)$$

This conditional symbol-error probability is shown in Fig. 1. The curves according to the original result for σ of [1] are shown in red. We conclude that higher constellations suffer from an error which is almost equal to the clipping rate. PAR reduction is essential to reduce the operating range of ampli ers and converters and thereby reducing the power dissipation, as long as no fully digital ampli ers are envisaged.

The least complex PAR (peak-to-average ratio) reduction scheme is certainly the so-called tone reservation method [3], [4]. In there, a certain share of carriers (typically 5 %) are reserved to generate a spiky "Dirac-like" function. This can be cyclically shifted to every time-domain position where a high peak occurs originating from the remaining data carriers. After shifting, the spiky function is subtracted using some weighting factor. In iterations, the peaks are stepwise reduced to a chosen threshold.

Part of this work was carried out while all authors had been with Telecommunications Research Center Vienna (ftw.).

[1] Strangely, very recent simulation results make us consider that the original formula for σ with a factor of 2 in the numerator may still be correct, since there seems to be a problem in the derivation of the average duration of clips τ_m, as well, although we cannot point out the error in the formal derivation, yet.

Partial transmit sequences (PTS) is due to Müller-Weinfurtner et al. [5] and is based on subdividing the frequency-domain in sub-blocks, each of which is separately IFFT transformed. Applying phase rotations to every block, the PAR of the summed time-domain signal is reduced. The rotations have to be selected by some optimization scheme. Apart from the IFFTs, this optimization scheme determines the complexity of the method and has up to now prevented the method to be applied in practical implementations.

A complexity reduction of PTS is possible by only allowing for 4 different phase rotations by multiples of 90° and by selecting the phase rotations according to a trellis structure, typically a 4-state trellis. This is then an intermediate method between a multidimensional trellis shaping as proposed in [6] and the original PTS. Both are based on sub-blocks with one reserved symbol per sub-block to detect the phase rotation or to include the shaping code. The complexity reduction of PTS when limiting the search to a trellis structure may make it a possible alternative to the oversampled tone reservation method.

In the following sections we will discuss tone reservation and provide updated simulation results to [4] and trellis-based PTS in some more detail.

II. Tone reservation

As has been mentioned, tone reservation reserves dimensions of the multicarrier signal in the DFT domain for peak reduction. In its lowest-complexity realization peaks in time domain are reduced by iterative subtraction of Dirac-like spiky functions $\mathbf{p}$, generated by the reserved carriers. The essential step is the iterative update

$$\mathbf{x}^{(i+1)} = \mathbf{x}^{(i)} - \alpha \cdot (x_m^{(i)} - \text{sign}(x_m^{(i)}) \cdot x_{target}) \cdot (\mathbf{p} \rightarrow m) \tag{6}$$

with a time-shifted version of $\mathbf{p}$ denoted $\mathbf{p} \rightarrow m$. m is the location of the peak in the time-domain signal. $(x_m^{(i)} - \text{sign}(x_m^{(i)}) \cdot x_{target})$ is the threshold overshoot and α a step size. Fortunately, the shift property of the DFT preserves the locations of the carriers reserved for the spiky function. The data carriers will thus not be disturbed.

α should grow with the PAR limit. Very high values of the step size α result in worse convergence, since sidelobes of the impulse-like vector p can more easily cause new peaks exceeding the relatively low threshold at other locations. The further the threshold is from the RMS value, the lower the chance is to generate a new value exceeding the threshold elsewhere. However, In practice, the choice of α is not critical.

Figure 2 shows the complementary cumulative frequency distribution, i.e., the probability of exceeding a given PAR[2].

Up to now, we described the real case named DMT, the base-band version of OFDM. However, the procedure can as well be used for complex signals. The update (6) has to be replaced by

$$\mathbf{x}^{(i+1)} = \mathbf{x}^{(i)} - \alpha \cdot (x_m^{(i)} - e^{j\text{arc}(x_m^{(i)})} \cdot x_{target}) \cdot (\mathbf{p} \rightarrow m) \ , \tag{7}$$

i.e., 'sign' has to be substituted by '$e^{j\text{arc}(.)}$'.

In order to take lter responses into account, an *oversampled* version of *tone reservation* is required. In [4] we proposed to realize the ne adjustment of shifts by the choice of suitable spiky update functions, which will actually be used in pairs, one for the oversampled and one for the non-oversampled rate. This enables to model the lter reponse in the oversampled path and in parallel processing the non-oversampled signal, which after processing will be fed through the real existing lter. It means that we will have L pairs of spiky functions where L is the oversampling factor.

One of the L vectors with the desired peak location (at the cancellation position) is selected in the oversampled domain and in parallel, the same selection and updating operation is performed with the corresponding vectors before oversampling. This procedure generates a time-domain signal in the original sampling rate that can then be fed into the real existing lter. For iterative subtraction, the necessary shift is split into a shift in the original non-oversampled spacing $\lfloor m/L \rfloor$ and the remaining shift of a fraction of the original spacing is realized by the choice within the set of L functions (index $(m \bmod L)$).
The nally resulting oversampled signal at the end of the iterations is usually not required, since the non-oversampled signal is to be fed through the real existing lter. Note that the iterative procedure is controlled by the oversampled ltered signal and the non-oversampled one is just computed together with it. As output, however, the non-oversampled and not ltered signal is required. The iterations are terminated when all samples' absolute values fall below the target level x_{target} or the maximum number of iterations i_{max} has been reached.

[2]The PAR de nition in here and also presumedly in Tellado's papers uses the average power of an unprocessed signal (with all carriers assumed to be active except for the unprocessed reference curve where the reserved carriers have been set to zero) as reference and is thus a direct measure for the peak voltage.

III. Average number of iterations in tone reservation

We estimate the probability for requiring an ith iteration. Hereto, we de ne

$$p = 2 \cdot Q(l) \ , \quad Q(x) = \frac{1}{\sqrt{2\pi}} \int_x^\infty e^{-t^2/2} dt \quad (8)$$

This is the exceedance probability for a given normalized threshold l. The addition of Dirac-like correction functions de nitely modify the frequency distribution. We tried to model this by an increase of the standard deviation by

$$\sigma_i = \sqrt{\sigma_{i-1}^2 + (x_{ci} \cdot \alpha)^2 / R_{D-PAR}}$$

with x_{ci} the average amplitude in the tail of the Gaussian density

$$x_{ci} = \frac{1}{\sqrt{2\pi} \cdot \sigma_{i-1}} \cdot \int_{l\sigma_{i-1}}^\infty x \cdot e^{\frac{-x^2}{2\sigma_{i-1}^2}} = \frac{\sigma_{i-1}}{2\pi} e^{-l^2/2} \ ,$$

and R_{D-PAR} the peak-to-average power ratio of the Dirac-like prototype function.

We found that this power increase would be much larger than experienced in practice. Thus, we considered the density to stay constant for every iteration.

For $\alpha = 1$, the processed peak will be completely reduced below the threshold. We then obtain that at least $i \geq \nu$ iterations need to be carried out with the probabilities $P_{\alpha\ldots}(i \geq \nu)$

$$\begin{aligned} P_{\alpha=1}(i \geq 1) &= 1 - (1-p)^N \\ P_{\alpha=1}(i \geq \nu) &\approx \sum_{i=\nu}^{N} \binom{N}{i} p^i (1-p)^{N-i} \\ &= 1 - \sum_{i=0}^{\nu-1} \binom{N}{i} p^i (1-p)^{N-i} \ , \end{aligned} \quad (9)$$

where N is the symbol length (FFT length). In case $0.5 \leq \alpha < 1.0$, we obtain additional terms

$$\begin{aligned} &P_{\alpha<1}(i \geq 1) = P_{\alpha=1}(i \geq 1) \\ &P_{\alpha<1}(i \geq \nu) \approx P_{\alpha=1}(i \geq \nu) + \\ &+ \textstyle\sum_{j=\lceil \nu/2 \rceil}^{\nu-1} \binom{N}{j} p^j (1-p)^{N-j} \ . \end{aligned} \quad (10)$$

For $\alpha < 1/2$ further terms would also have to be considered. This case is not of practical interest, anyway.

As an example, we considered l to be 11 dB. Figure 6 shows results from (9) and (10). The average number of iterations in Fig. 7 that can be computed from the distributions show a step function, which does not look brick-like just because we plotted in steps of 0.1. Figure 7 shows curves from $l = 8$ to 11 dB. Unfortunately, due to our simpli cations, the values do not match actual simulation results. However, the principle properties are clearly visible.

IV. Trellis PTS

PTS is based on subdividing the DFT-Block of length N into sub-blocks of length $B = N/N_B$ as shown in Fig. 4. Each time-domain component vector $\mathbf{x}_i$ is computed as

$$\mathbf{x}_i = \text{IFFT}(\mathbf{X}_i) \ , \quad i = 1, \ldots, N_B \quad (11)$$

and the nal time-domain signal will be computed by summing up all rotated component vectors,

$$\mathbf{x} = \sum_{i=1}^{N_B} b_i \cdot \mathbf{x}_i = \sum_{i=1}^{N_B} e^{j\varphi_i} \cdot \mathbf{x}_i \ . \quad (12)$$

Note that the conjugate phase rotations in Fig. 4 are due to the conjugacy constraints of DMT (baseband OFDM). Earlier results by Müller-Weinfurtner et al. have shown that four different phases per block suf ce. Recently, we have found that selecting the phases according to a trellis of a convolutional code with 5 and 7 as the octal generators can be used to further reduce the complexity of the method. The rotation phases corresponding to every trellis path have to be selected such that the phase differences are maximized when paths emanate from a common state or merge into one state. This means one nds 0° and 180° or 90° and 270° at the paths emanating or reaching a state. This is just the usual construction principle of convolutional or trellis codes. In the case of the best convolutional codes, it is the Hamming distance that is maximized when paths split or merge. We do the standard intermediate decisions when paths merge as is done in the Viterbi algorithm. This trellis approach is actually the same as trellis shaping [6], [7], except that we do not apply syndrome and inverse syndrome formers.

We studied block lengths of 2,4,8, and 16. Assuming that we require to reserve one complete component per block for phase detection at the receiver, the corresponding redundancies would be 0.5, 0.25, 0.125, and 0.0625, respectively. The latter is only slightly more than the typical value that we chose for tone reservation. Results of the clipping probability over the PAR are given in Fig. 5 and show that the method has a similar performance as tone reservation and can thus be considered as an alternative although

the complexity is still higher due to the IFFTs of the sub-blocks.

V. Performance results

The performance results shown here use a Butterworth lter of order 6 and a 3-dB edge frequency at 1.104 MHz (clock rate 2.208 MHz) including the $\sin(x)/x$ sample-and-hold roll-off. The non-oversampled original tone reservation yields Fig. 2, where we show the ideal non-oversampled result together with the distribution after ltering. Even with the soft roll-off of the chosen Butterworth lter, most of the PAR reduction gain is gone.

Note that the Butterworth lter does not strictly limit the band according to the sampling theorem. A time-shift results in a rotation in the DFT domain, if we consider extended vectors according to the oversampling. A phase rotation in the non-extended DFT-domain vector cannot represent rotations in alias bands. This causes differences in the shape of the L shifted versions of the Dirac-like functions. The impulses at the output of the Butterworth lter do not always show the desired optimum locations of the peaks (aliasing). This may be controlled by modifying the rotation.
The corresponding vectors at the input of the lters are even further from the equidistant spacing. However, the Dirac-like properties and correct positions are required at the output of the lter, not at the input.

Figure 3 shows the results with the proposed oversampled parallel procedure. Most of the reduction gain is maintained. In both gures, two different threshold values (8 and 9.5) have been used, but they differ only slightly at a probability of 10^{-7}. Note that this value is the desired bit-error rate for an ADSL line. This is the reason for requiring the clipping probability to be less than 10^{-7}.

We should mention that edge effects due to the blocked modeling of a continuous lter will slightly reduce the PAR reduction gain, which is not shown in this paper. These effects will be outlined in a later publication. We always show distributions at the 40th iteration. However, 10 iterations should be suf cient in practice.

Performance results for trellis PTS are given in Fig. 5. Comparing gures 2 and 5, the non-oversampled ideal curves, we observe that the gains are not too different for both schemes. Complexity is lower in the case of tone reservation, but trellis PTS may still be a worthwhile alternative.

VI. Conclusions

We have described an oversampled variant of tone reservation based on a parallel structure with non-oversampled and oversampled branches. Additionally, we presented complexity-reduced PTS (partial transmit sequences) selecting the phase rotations from a trellis. Both methods deliver comparable performances and are the procedures that are most suitable for practical implementations.

References

[1] A.R.S. Bahai, M. Sigh, A.J. Goldsmith, and B.R. Saltzberg, "A new approach for evaluating clipping distortion in multicarrier systems," *IEEE JSAC*, vol. 20, no. 5, pp. 1037-1046, June 2002.

[2] Henkel, W., Azis, V., Trautmann, S., "The analytic treatment of the error probability due to clipping — a solved problem?" *ISITA 2004*, Parma, Italy, October 10–13, 2004.

[3] Tellado, J., "Peak-to-Average Power Reduction for Multicarrier Modulation", *Dissertation*, Stanford University, Sept. 1999.

[4] Henkel, W., Zrno, V., "PAR Reduction Revisited: An Extension to Tellado's Method," *6th International OFDM-Workshop*, Hamburg, Sept. 18-19, 2001.

[5] Müller, St.H., Bäuml, R.W., Fischer, R.F.H., Huber, J.B., "OFDM with Reduced Peak-to-Average Power Ratio by Multiple Signal Representation", *Annals of Telecommunications*, Vol. 52, No. 1-2, Feb. 1997, pp. 58-67.

[6] Henkel, W., Wagner, B., "Another Application for Trellis Shaping: PAR Reduction for DMT (OFDM)," *IEEE Trans. on Comm.*, Vol. 48, No. 9, pp. 1471-1476, Sept. 2000.

[7] Forney, G.D., "Trellis Shaping", *IEEE Trans. on Information Theory*, Vol. IT-38, No. 2, pp. 281-300, March 1992.

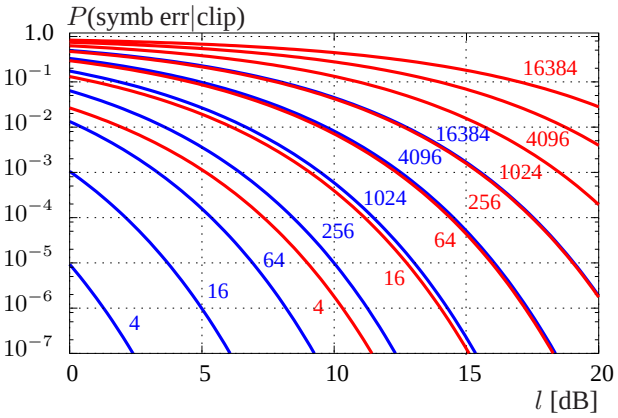

Fig. 1. Symbol-error probability in a clip ($N = 512$, M given as parameter)

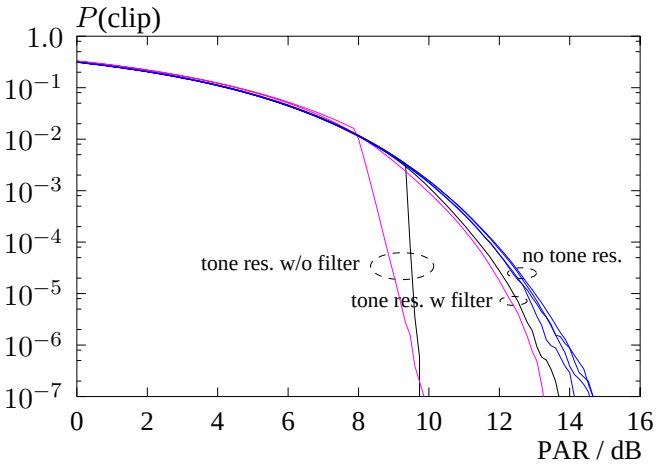

Fig. 2. Complementary cumulative frequency distributions over the PAR for Tellado's original procedure without oversampling before and after ltering; the 40th iteration is shown

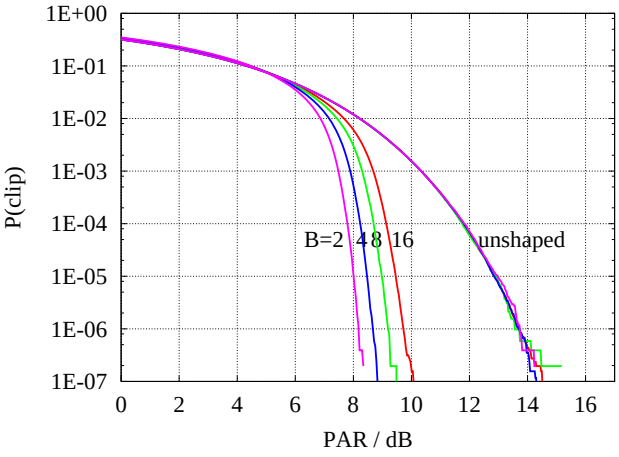

Fig. 5. The probability of clipping applying trellis PTS (not oversampled)

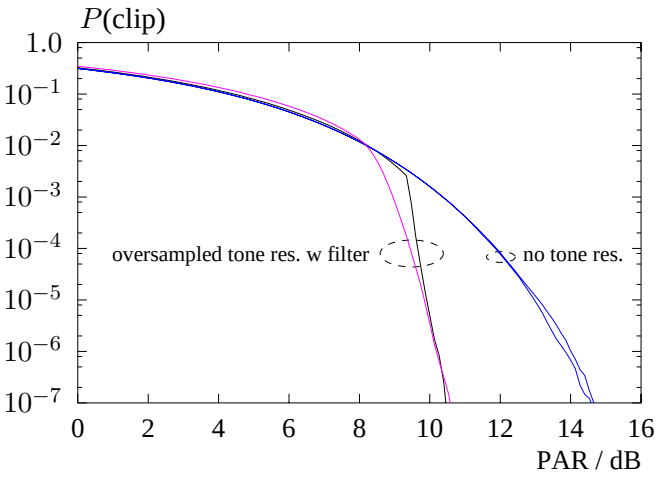

Fig. 3. The complementary cumulative frequency distributions over the PAR for the parallel oversampled procedure (40th iteration)

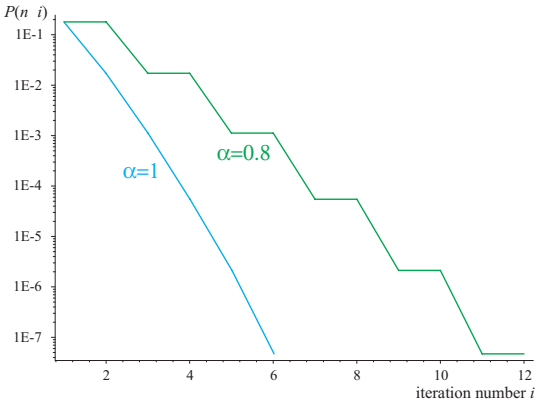

Fig. 6. Probability of requiring i iterations for $\alpha = 0.8,\ 1$

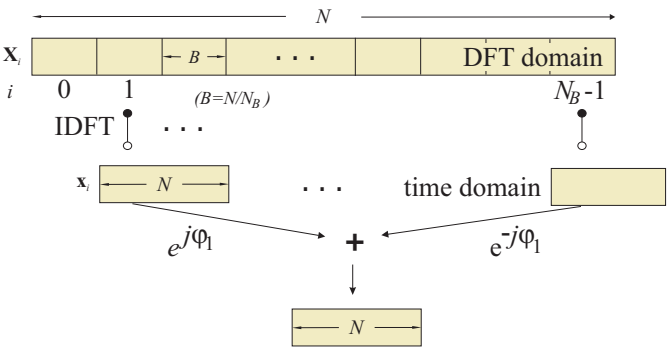

Fig. 4. PTS phase rotations in the case of DMT

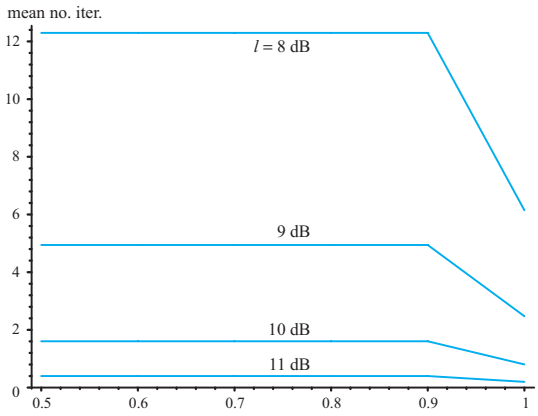

Fig. 7. Average number of Tellado iterations dependent on α